doi: 10.12029/gc20220107003

何建华,曹峰,邓虎成,王园园,李勇,徐庆龙. 2023. 四川盆地HC地区须二段致密砂岩储层地应力评价及其在致密气开发中的应用[J]. 中国地质, 50(4): 1107−1121.

He Jianhua, Cao Feng, Deng Hucheng, Wang Yuanyuan, Li Yong, Xu Qinglong. 2023. Evaluation of in−situ stress in dense sandstone reservoirs in the second member of Xujiahe Formation of the HC area of the Sichuan Basin and its application to dense sandstone gas development[J]. Geology in China, 50(4): 1107−1121(in Chinese with English abstract).

四川盆地HC地区须二段致密砂岩储层地应力评价及其在致密气开发中的应用

何建华[1,2],曹峰[1],邓虎成[1,2],王园园[3],李勇[1],徐庆龙[4]

(1.成都理工大学能源学院,四川 成都 610059;2.油气藏地质及开发工程全国重点实验室(成都理工大学),四川 成都 610059;
3.中海石油(中国)有限公司海南分公司,海南 海口 570100;4.大庆油田有限责任公司勘探开发研究院,黑龙江 大庆 163000)

提要:【研究目的】四川盆地HC地区须二段勘探开发潜力巨大,但该地区为典型的低孔低渗致密气藏,需要进行地应力精细评价来为后期纵向上压裂选层和平面上工程甜点区优选提出建议进而提高产能。**【研究方法】**基于25组声发射和13组差应变等实验测试分析,结合水压致裂、常规和特殊测井资料,进行地应力的精细评价,以期分析在致密砂岩储层中不同实验测试方法的适用性,查明有利于工程改造的层位和甜点区。**【研究结果】**实验测试结果表明HC地区须二段最大水平主应力值为50.77~75.65 MPa,均值为59.71 MPa;最小水平主应力值为45.37~54.31 MPa,均值为49.31 MPa;垂向主应力为48.11~65.62 MPa,均值为56.53 MPa。模拟结果表明储层内部应力隔层厚度和两向应力差异系数越小,越有利于压裂改造。通过对比小层间的三向应力关系,表明须二段处于走滑应力状态。HC地区须二段致密砂岩均质性较强,声发射测试结果误差较大,差应变测试结果与其他地应力大小解释结果具有更高一致性,故该测试方法更加适用于均质性较强的砂岩地层。**【结论】**结合地应力大小,纵向上建议选择隔层组合更有利的须二2亚段中上部为压裂目的层;且为了达到较好的体积缝网压裂改造效果,平面上建议避开两向应力差异系数较大的断层附近区域,应选择优质储层发育且水平应力差异系数相对较小的HC地区中部HC102−HC111井区。

关 键 词:致密气;地应力大小;声发射测试;差应变测试;油气勘查工程;须二段;HC地区;四川盆地

创 新 点:揭示了差应变测试相比于声发射测试更加适用于均质性致密砂岩储层地应力大小测量;隔层应力结构与水平应力差异系数共同控制了HC地区须二段“工程甜点”的分布。

中图分类号:P618.13 **文献标志码:**A **文章编号:**1000−3657(2023)04−1107−15

Evaluation of in−situ stress in dense sandstone reservoirs in the second member of Xujiahe Formation of the HC area of the Sichuan Basin and its application to dense sandstone gas development

HE Jianhua[1,2], CAO Feng[1], DENG Hucheng[1,2], WANG Yuanyuan[3], LI Yong[1], XU Qinglong[4]

收稿日期: 2022−01−07;**改回日期:** 2022−04−05

基金项目:深地科学与工程教育部重点实验室开放基金(DESEYU 202102)和四川省科技厅重点苗子项目(2022JDRC0103)联合资助。

作者简介:何建华,男,1990年生,副研究员,主要从事非常规油气储层天然裂缝成因机制与定量表征、地应力场精细描述研究工作;E−mail: hejianhuadizhi@163.com。

(1. *College of Energy, Chengdu University of Technology, Chengdu* 610059, *Sichuan, China;* 2. *National Key Laboratory of Oil & Gas Reservoir Geology and Exploitation, Chengdu University of Technology, Chengdu* 610059, *Sichuan, China;* 3. *Haikou Branch of CNOOC Ltd, Haikou* 570100, *Hainan, China;*4. *Exploration and Development Research Institute, Daqing Oilfield Company Ltd., Daqing* 163000, *Heilongjiang, China*)

Abstract: This paper is the result of oil and gas exploration engineering.

[Objective]The second member of Xujiahe formation of the HC area in the Sichuan Basin has great potential for exploration and development, but it is a typical low-porosity and low-permeability tight gas reservoir, which requires in-situ stress refined evaluation to recommend the optimal selection of engineering sweet spots for later vertical fracturing and plane fracturing to increase production. **[Methods]** Based on experimental test analysis such as 25 groups of acoustic emission and 13 groups of differential strain, combined with hydraulic fracturing, conventional and special logging data, we analyze the applicability of different experimental test methods in tight sandstone reservoirs by performing a fine-scale evaluation of in-situ stress and identified layers and sweet spots conducive to engineering modifications. **[Results]**The results of the experimental tests of the second member of Xujiahe formation in the HC area showed that the maximum horizontal principal stress values ranged from 50.77 to 75.65 MPa, with a mean value of 59.71 MPa; the minimum horizontal principal stress values ranged from 45.37 to 54.31 MPa, with a mean value of 49.31 MPa; and the vertical stress values ranged from 48.11 to 65.62 MPa, with a mean value of 56.53 MPa. The simulation results show that the smaller the thickness of the stress barrier within the reservoir and the differential coefficient of in-situ stress in both directions, the more favorable the fracture modification. The comparison of the three-dimensional stress relationships between the minor layers indicates that the second member of Xujiahe Formation is in a strike-slip stress state. The dense sandstone in the second member of the Xujiahe Formation is more homogeneous, the acoustic emission test results are more inaccurate. The results of the differential strain test are in better agreement with the results of the in-situ stress magnitude interpretation, making the test method more suitable for more homogeneous sandstone formations. **[Conclusions]** In combination with the magnitude of in-situ stress, it is recommended vertically that the more favorable combination of compartments, upper middle of the second subsection of Xu-II, be selected as the target layer for fracturing. To achieve a better volume fracturing network, it is recommended to avoid areas near faults with a large differential coefficient of two-dimensional stress. The area of HC102-HC111 well in the central part of the HC area, where high-quality reservoirs are developed and two-dimensional stress difference factor is relatively small, should be selected.

Key words: tight gas; magnitude of in-situ stress; acoustic emission test; differential strain test; oil and gas exploration engineering; the second member of Xujiahe Formation; HC area; Sichuan basin

Highlights: This study reveals that differential strain testing is more suitable for measuring the magnitude of in-situ stress in homogeneous tight sandstone reservoirs than acoustic emission testing; The distribution of 'engineering dessert' in the second section of Xujiahe Formation in HC area is both controlled by the interlayer stress architecture and horizontal stress difference coefficient.

About the first author: HE Jianhua, male, born in 1990, associate professor, mainly engaged in the mechanism and quantitative characterization of natural fractures in unconventional oil and gas reservoirs and the fine description of the in-situ stress field; E-mail: hejianhuadizhi@163.com.

Fund support: Supported by the Open Found from Key Lab of Deep Earth Science and Engineering, Ministry of Education (No. DESEYU202002), Sichuan Provincial Science and Technology Department Key Seedling Project (No. 2022JDRC0103).

1 引 言

随着常规油气资源的不断消耗,非常规油气资源的勘探及大规模高效开发成为国家重大战略需求;致密砂岩气作为非常规天然气的重要类型,是常规天然气资源的最重要的后备补充之一,并将在今后的10~20年成为中国天然气开发利用的主体资源之一,在中国非常规天然气勘探开发中发挥先导作用(丁文龙等,2015;朱宏权等,2019)。中国自从发现川西中坝气田之后,逐步系统开展了致密砂岩气藏的勘探和开发研究,且发现四川盆地陆相致密砂岩气资源十分丰富;近年来,中国又在川中地区

相继发现了合川、安岳两个以须二段为主要产气层的千亿级大气田,这展现了川中地区须家河组良好的勘探开发前景(李国辉等,2012;聂舟,2018;郑和荣等,2021)。目前川中地区是四川盆地须家河组天然气主产区,其日产气量超过160×10^4 m^3,占盆地须家河组64%;而川中地区须二段天然气探明储量近4500×10^8 m^3,占整个川中地区须家河组探明储量的75%,川中地区须二段累产气量近90×10^8 m^3,占川中地区须家河组累产气量的70%,由此可见川中地区须二段是四川盆地须家河组天然气勘探生产的主要产层段(赵正望等,2019)。虽然HC地区须家河组勘探表明储层具有较大的天然气储量资源,开发前景巨大,但储层地质特征复杂,属于典型的低孔、低渗的难采气藏,所以亟需进行地应力研究来提高气藏改造效果、完善增产作业措施。

地应力是指客观赋存于地壳岩体内且未受工程扰动的一种自然力,亦称原岩应力,其主要由重力应力、构造应力、孔隙压力、热应力和残余应力等耦合而成(纪志久等,2009;张重远等,2012;赵亚军和孟楠楠,2015)。地应力对矿山开采、地下工程和能源开发等生产实践均起着至关重要的作用(郭伟杰等,2010)。地应力的测量方法从测量原理上可分为地应力直接测量法和地应力间接测量法,直接测法通过扰动岩石的初始条件,以产生应变、变形、裂隙张开等,如水压致裂法和声发射法等;间接地应力测量是基于对与地应力有关现象分析,如应力解除法和应变恢复法等(蔡美峰,1993;景锋等,2008;梁晨,2020)。若将其按照数据来源进行归类则可以分为五大类,即基于岩心的方法、基于钻孔的方法、地质学方法、地球物理方法、基于地下空间的方法(王成虎,2014)。针对HC地区须二段致密砂岩储层的地应力评价研究,分别利用声发射测试和差应变测试进行地应力大小测量。声发射法是通过岩石凯塞尔效应测定深部岩体地应力,以寻求区域性地应力变化规律,与传统的应力解除法、水力压裂法相比,具有简单、直观、相对经济等优点,便于大量测试(姜永东等,2005;Lehtonen et al.,2011;Liu et al.,2019);但也存在测试结果精度不高、现今地应力Kaiser效应点识别困难的问题(Jayanthu,2019;Fraser et al.,2021)。而差应变分析法则通过测试模拟地层条件下岩心各方向的应变差,即可知道这块岩心在地层中所受的应力状态(沈海超等,2008)。

地应力的大小及变化在油藏整个开发过程中都具有极其重要的作用,是控制油气富集区域的分布、储层裂缝的展布、地层破裂压力、坍塌压力等多项参数的重要因素之一;其也是油气勘探开发过程中方案制定和工程设计必不可少的依据,并对采注井网的布置、注水开发设计、油气富集区预测、射孔方案确定、油井压裂设计、开采过程中油井出砂问题、钻井套管的变形问题、井壁的稳定性等方面都有重要影响(刘泽凯等,1994;王宏伟,2007;马睿,2014;曹慧等,2020)。本文通过两种实验方法对地应力大小进行测量,并利用水压致裂法和测井资料对实验测量结果进行评价,通过对比分析得出测量方法优选建议,并将地应力评价结果应用于HC地区须二段致密砂岩开发中,为纵向上压裂选层及平面上压裂"甜点区"的优选提供建议。

2　样品制备与实验方法

利用声发射测试和差应变测试对样品进行地应力大小实验测试分析,声发射测试需在与钻井岩心轴线垂直的水平面内,增量为45°的方向上钻取3块岩样,并测出其3个方向的正应力,而后求出最大水平主应力、最小水平主应力;其实验样品需加工成25 mm×50 mm的圆柱形试样,并将圆柱形试样两端车平、磨光,两端面的不平行度小于0.015 mm,然后即可对研究区10口井的25组样品进行试验;声发射测试的原理是脆性材料对曾经受过的载荷作用具有记忆性,利用岩石这一特性,在室内实时记录岩石在单轴载荷不断增加的情况下,岩石在不同载荷水平下产生的声发射信号,根据声发射信号的几个突变点确定不同级别的应力分量(姜永东等,2005)。为了更准确地测试声发射Kaiser点对应的应力值,进行围压下的声发射Kaiser实验,获得了围压下Kaiser点应力与围压之间的关系式如公式(1):

$$\sigma_{pc}=f(\sigma_0,P_c) \tag{1}$$

式中:P_c为围压,σ_{pc}为围压条件下的Kaiser点应力,σ_0为真实有效应力值,f为关系式。

差应变测试需将现场取回的岩心加工成50 mm×50 mm×50 mm的立方体试样(图1),并在相互垂直的三个表面各贴上一组应变片花。将试样

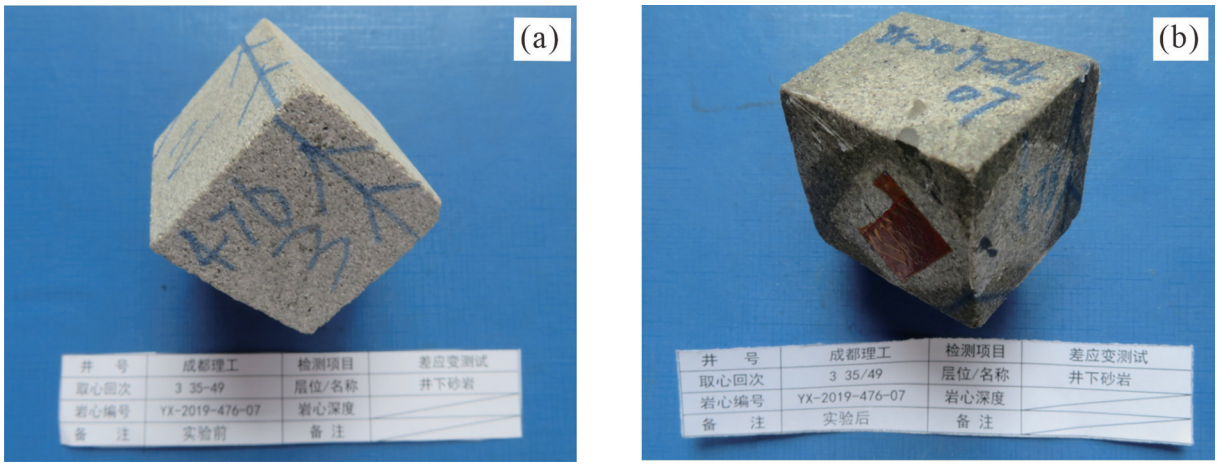

图1 差应变实验测试前后样品照片

a—差应变实验前样品照片;b—差应变实验后样品照片

Fig. 1 Photos of samples before and after the differential strain test

a−Photograph of sample before differential strain test; b−Photograph of sample after differential strain test

用硅橡胶密封后放入压力容器中施加静水压力,直到超过预计原地应力,此时微裂隙将完全闭合。通过样品表面的9个应变片测量微裂隙闭合前后该方向的应变变化,计算出基于岩心坐标系的6个应变分量,并根据弹性力学计算出三个主应力的比值,再利用微裂隙闭合点的压力作为最大水平主应力或根据样品岩心所在的深度推算垂向主应力的大小,最后结合主应力比值估算出该处三向地应力大小(韩军和刘洪涛,2005)。

3 基于岩心实验测试评价地应力大小

3.1 声发射实验测试

声发射测试的原理是脆性材料对曾经受过的载荷作用具有记忆性,通过对岩石试件进行单轴压缩试验,同时测定试件在受压过程中产生的声发射信号,根据声发射信号的几个突变点确定不同级别的应力分量(图2)。

25组井下样品地应力测试结果表明最大水平主应力值为50.77~75.65 MPa,均值为59.71 MPa;最小水平主应力值为45.37~54.31 MPa,均值为49.31 MPa;垂向主应力值为48.11~65.62 MPa,均值为56.53 MPa(表1)。将四川盆地不同构造区须二段地应力大小进行比较发现:HC地区的地应力测试结果与具有相当深度川东北河坝地区的测试结果具有一致性(图3)。而须二段还可细分为须二1亚段、须二2亚段及须二3亚段三个小层,将各小层的最大水平主应力、最小水平主应力和垂向主应力进行对比发现:三向应力之间具有最大水平主应力>垂向主应力>最小水平主应力的特征,属于Ⅲ类地应力类型,处于走滑应力状态(赵景辉等,2021);且须二段由下至上,三向应力值逐渐减小。

3.2 差应变实验测试

差应变实验过程中直接采集到的是在岩样上相邻的、相互正交的3个面上9个方向的应变(何小东等,2020),并根据弹性力学计算出三个主应力的比值,用微裂隙闭合点的压力作为最大主应力或根据样品岩心所在的深度推算垂直应力的大小,最后结合主应力比值估算出该处三向地应力大小(图4)。

差应变实验所得的三向应力结果表明,最大水平主应力值为54.57~64.94 MPa,均值为59.26 MPa。最小水平主应力值为46.3~56.67 MPa,均值为51.51 MPa。垂向主应力为52.87~60.93 MPa,均值为57.08 MPa(表2)。三向应力之间的特征也为最大水平主应力>垂向主应力>最小水平主应力,处于走滑应力状态。

3.3 水压致裂评价地应力大小

利用水压致裂法来进行现场地应力测量主要是依据整个压裂施工过程中记录下的压力随时间变化的曲线,结合有关的岩石力学参数及压裂理论,进而求出地应力大小。与其他测量方法相比,

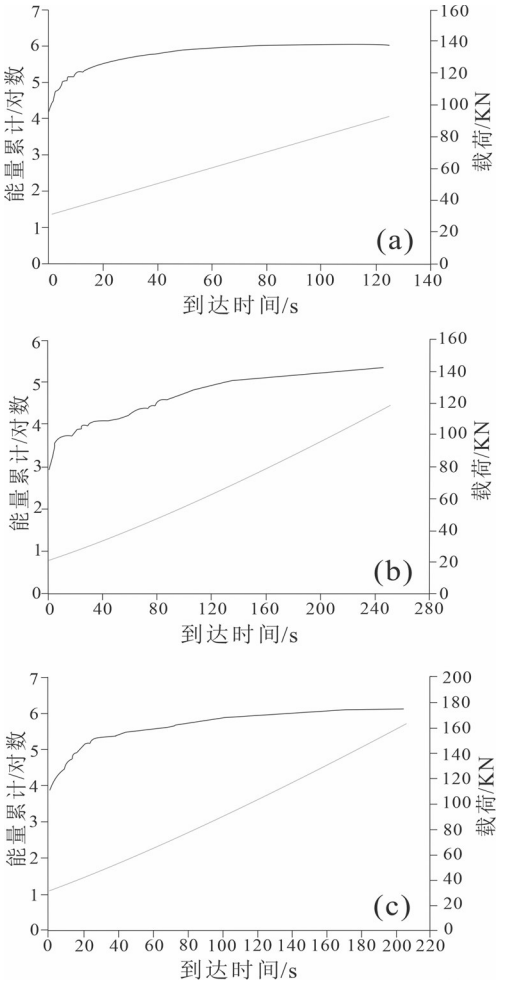

图2 声发射实验结果图

a—HC137井须二1亚段2281.5 m样品声发射曲线;b—HC001-27-x1井须二2亚段2438.05 m样品声发射曲线;c—HC5井须二3亚段2231.1 m样品声发射曲线

Fig. 2 Acoustic emission test results

a-Acoustic emission profile of a 2281.5 m sample from the first subsection of Xu-II of well HC137; b-Acoustic emission profile of a 2438.05 m sample from the second subsection of Xu-II of well HC001-27-x1; c-Acoustic emission profile of a 2231.1 m sample from the third subsection of Xu-II of well HC5

其无需知道岩体的力学参数,即可获得地层中现今地应力的多种参量,且具有设备简单、操作方便、测量深度深,可在任意深度进行连续或重复测试、测量速度快、测值直观、测值代表性大等诸多优点(刘亚群等,2007;赵刚和董事尔,2009;Schmitt et al.,2012;王成虎等,2020);利用压裂施工资料确定地应力的方法是目前最直接、最可靠的方法之一。

通过对压裂资料的整理分析和计算(图5),认为须二段的泵压较高,主要分布在59~70 MPa,平均为64.25 MPa,表明岩石较为致密,压开具有一定的难度;依据施工参数数据计算的地应力大小结果,发现其具有最大水平主应力>垂向主应力>最小水平主应力的大小关系,综合分析认为该地区须家河组地层为走滑地应力类型,这与声发射实验及差应变实验的测试结果都较为一致。

利用压裂资料进行计算,得出水压致裂法计算的地应力大小数据结果(表3),以HC001-69井为例,其最大水平主应力为56.43 MPa,最小水平主应力为46.43 MPa,垂向主应力为53.48 MPa。而分别将声发射实验和差应变实验在HC001-69井同层位相当深度情况下的测试结果与利用水压致裂法计算的结果相对比来看,声发射实验所测得的结果明显更大,而差应变实验所得的结果与水压致裂计算所得结果更为相近。

4 基于常规和特殊测井资料评价地应力大小

4.1 井眼崩落宽度反演地应力大小

利用井壁垮塌的结构恢复方法,可反演出现今地应力大小结果(图6)。其中应力多边形可以描述给定深度、断层摩擦系数以及孔隙压力情况下所确定的最大水平主应力与最小水平主应力可能的取值范围(王璞等,2019)。两条红色斜线表示由钻孔崩落张开角度WBO及有效岩体抗压强度(EUCS)确定的应力量值约束条件,最小EUCS的上方与最大EUCS下方区域表示估计应力量值(陈念等,2021)。

以HC001-69井为例,通过计算得到该层位最大水平主应力的范围为51.8~57.3 MPa,最小水平主应力的范围为45.4~47.3 MPa;在HC001-69井的同层位相当深度情况下,声发射测试所得最大水平主应力接近60 MPa,最小水平主应力也比较大,而差应变测试所得的最大水平主应力和最小水平主应力都在反演地应力大小所得结果的范围以内。由此表明声发射测试结果误差较大,差应变测试结果更为准确。利用上述结论可对地应力大小测试方法进行优选,即差应变测试更适用于须家河组均质性致密砂岩。

4.2 交叉偶极子阵列声波测井评价地应力大小

利用实验方法测定地应力时,因其测量数量有

表1 HC地区须家河组声发射实验测试的三向应力值的测试结果数据表(部分)

Table 1 Results of three-dimensional stress values of the second member of Xujiahe Formation in HC area by acoustic emission test

井号	层位	井深/m	岩性	Kaiser点应力值/MPa				最大水平主应力/MPa	最小水平主应力/MPa	垂向主应力/MPa
				0°	45°	90°	垂直			
HC001-69	须二2	2129.05~2129.30	中砂岩	37.49	32.84	35.35	43.27	55.36	47.89	54.75
HC001-69	须二2	2144.40~2146.35	中砂岩	38.56	32.53	33.49	45.58	59.67	47.04	58.79
HC001-69	须二2	2156.85~2158.10	粉砂岩	44.99	31.84	33.06	51.54	63.77	45.09	61.99
HC109	须二2	2214.60~2215.70	细砂岩	41.55	33.57	37.29	35.71	59.92	47.47	49.98
HC5	须二3	2230.90~2231.20	中砂岩	39.89	36.56	37.56	39.84	55.56	50.64	54.21
HC001-27-x1	须二2	2404.80~2407.05	中砂岩	38.00	32.92	33.94	43.63	58.93	49.72	57.05
HC001-27-x1	须二2	2412.05~2414.20	中砂岩	41.12	33.63	40.63	45.87	65.49	49.21	61.05
HC001-27-x1	须二2	2418.15~2419.05	细砂岩	46.79	38.45	39.11	47.74	66.14	50.97	62.98
HC001-27-x1	须二2	2431.85~2432.30	粉砂岩	47.88	35.2	38.06	58.93	69.35	52.49	64.6
HC137	须二1	2281.05~2281.50	中砂岩	40.52	34.89	38.51	42.35	58.94	49.48	57.04
HC001-69	须二3	2102.85~2103.05	细砂岩	36.44	32.58	35.95	39.02	53.37	46.12	52.57

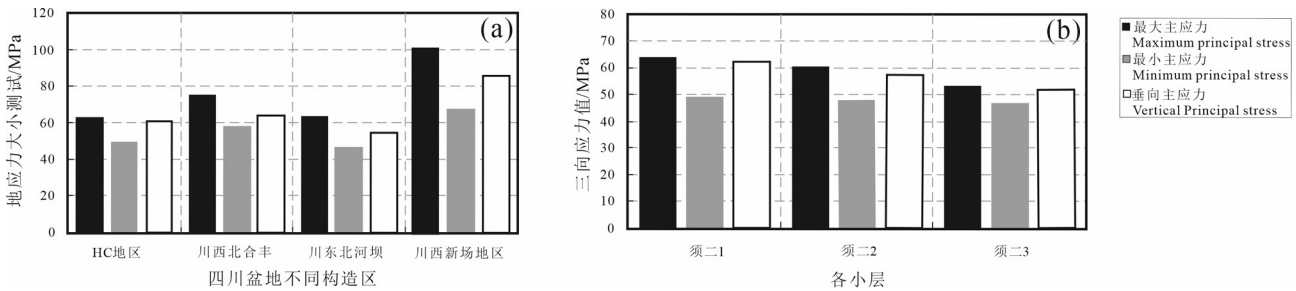

图3 须二段地应力大小统计图

a—四川盆地不同构造区须二段地应力大小统计图;b—HC001-69井须二段各小层样品地应力大小统计图

Fig.3 Statistical map of the magnitude of in-situ stress in the second member of Xujiahe Formation

a-Statistical map of the magnitude of in-situ stress in different tectonic zones of the Sichuan Basin in the second member of Xujiahe formation; b-Statistical map of the magnitude of in-situ stress in each sub-layer sample from the second member of Xujiahe Formation of well HC001-69

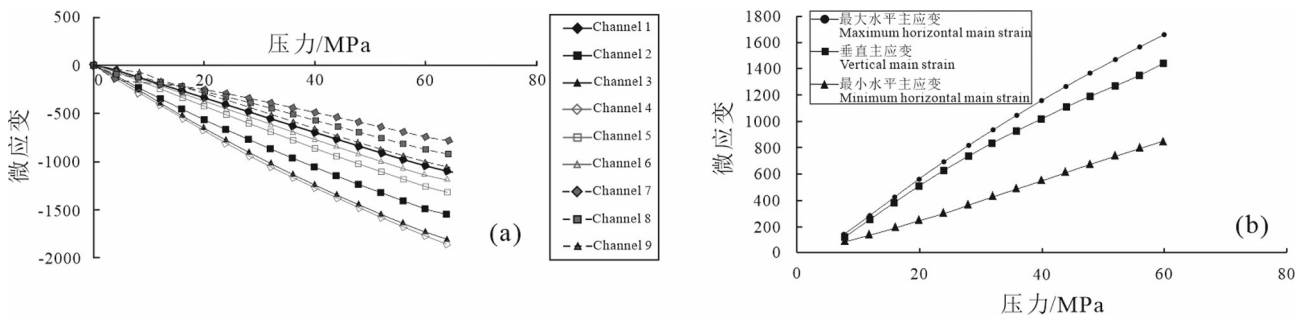

图4 差应变实验中主应力比值随着围压变化曲线图,HC001-27-x1,2404.8 m

a—岩心9通道主应力比值随围压变化曲线;b—岩心主应力比值随围压变化曲线

Fig.4 Variation of principal stress ratio with surrounding pressure in differential strain experiments, HC001-27-x1, 2404.8 m

a-Variation of principal stress ratio with surrounding pressure for 9 channels in the core; b-Variation of core principal stress ratio with the surrounding pressure

表2 HC地区须二段差应变实验测试的三向应力值的测试结果

Table 2　Results of three-dimensional stress values of the second member of Xujiahe Formation in HC area by differential strain test

井号	层位	深度/m	三向主应力值/MPa		
			最大水平主应力	最小水平主应力	垂向主应力
HC001-27-x1	须二2	2414.2	62.70	53.35	60.40
HC001-27-x1	须二2	2434.6	63.30	54.30	60.86
HC001-27-x1	须二2	2404.8	62.77	53.87	60.12
HC001-69	须二2	2155.5	54.76	46.77	53.89
HC001-69	须二2	2143.5	54.66	46.30	53.67
HC109	须二2	2214.6	58.46	52.71	55.36
HC5	须二3	2230.9	56.50	48.63	55.77
HC1	须二3	2115	54.57	49.5	52.87
HC001-27-x1	须二2	2419	63.14	54.19	60.48
HC001-27-x1	须二2	2432.3	64.94	56.67	60.81
HC001-27-x1	须二2	2437	64.33	56.54	60.93
HC001-69	须二2	2144.4	55.54	48.68	53.61
HC001-69	须二2	2130.1	54.74	48.10	53.25

限,导致不能获得连续的地应力剖面;而测井资料具有连续性好,分辨率高的特点,因此可通过测井资料获得连续的地应力剖面(Mao et al.,2019)。本次测井解释地应力大小利用的是ADS方法,其适用于砂泥岩地层,对具有$\sigma_H<\sigma_v<\sigma_h$的三向应力关系的地层效果较好,且已在川西新场地区和川西北合丰地区取得较好的应用效果。其基本原理如公式(2):

$$\begin{cases}\sigma_v=\int_0^H\rho(h)\cdot g\cdot dh\\ \sigma_x=\mu_g\dfrac{\upsilon}{1-\upsilon}\sigma_v+\mu_g\dfrac{1-(1+\mu_g)\upsilon}{1-\upsilon}(1-\dfrac{C_{ma}}{C_b})P_p\\ \sigma_y=\dfrac{\upsilon}{1-\upsilon}\sigma_v+\dfrac{1-2\upsilon}{1-\upsilon}(1-\dfrac{C_{ma}}{C_b})P_p\end{cases}\tag{2}$$

式中:σ_x、σ_y为x、y方向水平应力,MPa;σ_v为垂向应力,MPa;μ_g为地层水平骨架应力的非平衡因子,无量纲;υ为泊松比,无因次;P_p为孔隙压力,MPa;C_{ma}、C_b为岩石骨架压缩、岩石体积压缩系数。

其中,μ_g可以利用双井径资料获取,即用井眼的应力变形来反映构造应力的变化,计算如公式(3):

$$\mu_g=1+k\left[1-(\frac{d_{min}}{d_{max}})^2\right]\frac{E_b}{E_{ma}}\tag{3}$$

式中:d_{min}、d_{max}分别为测点井眼直径的最小、最大值,cm;E_b、E_{ma}分别为岩石、岩石骨架的杨氏模量,MPa;k为刻度系数。

利用常规测井声波时差及补偿密度测井资料计算出地层动态泊松比、上覆岩层重量等力学参数

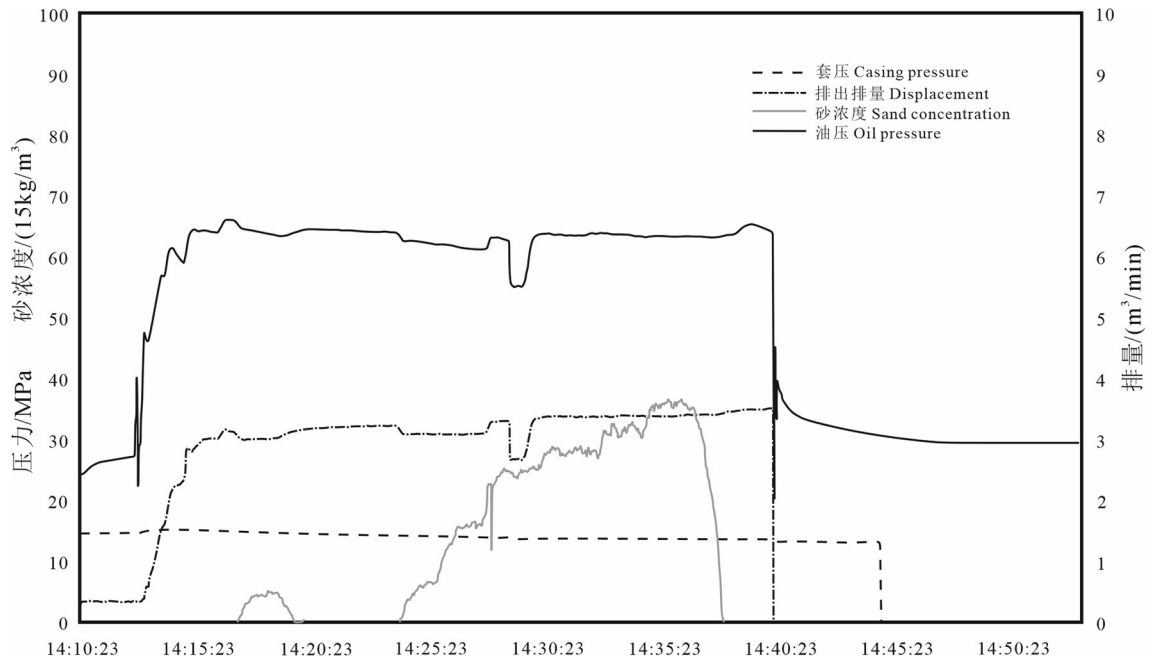

图5　HC001-6-X3井上层压裂施工曲线图

Fig.5　Construction curve of the upper fracture of well HC001-6-X3

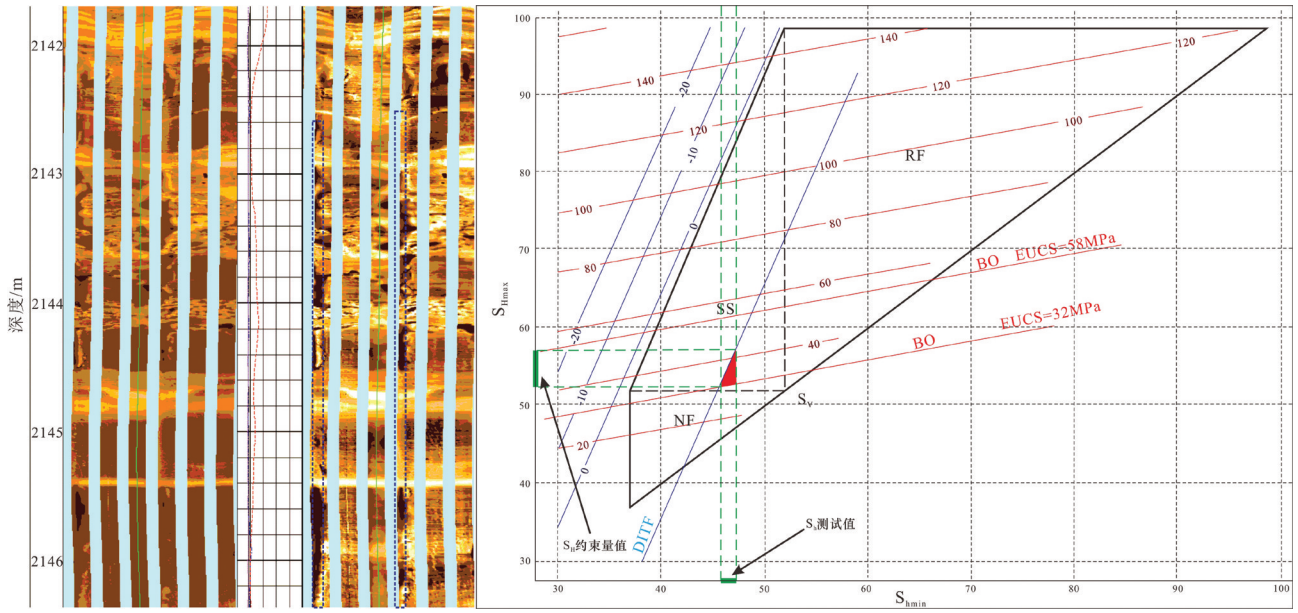

图6 HC001−69井井壁垮塌反演地应力大小图

Fig.6 Estimated in−situ stress magnitude of well wall collapse in well HC001−69

表3 水压致裂法计算的地应力大小的数据结果

Table 3 Results of the magnitude of in−situ stress calculated using hydraulic fracturing

井号	层位	井深/m	最大水平主应力/MPa	最小水平主应力/MPa	垂向主应力/MPa
HC001-6-x3	须二2	2370.6~2377	62.99	53.58	57.05
HC001-21-x1	须二2	2298~2316	60.89	51.2	56.15
HC001-5-x3	须二2	2278~2280	59.68	47.34	55.67
HC001-69	须二2	2141.32	56.43	46.43	53.48

后，可以通过测井资料间接计算现今地应力值（Wang et al.，2021）。测井资料求取地应力方法方便且易于推广，但这种间接的计算方法与实际的地应力值具有一定的偏差，需要利用其他方法对其结果进行校正（井壁崩落法、差应变法、压裂法等）。

测井计算的各小层三向应力值与实测值的吻

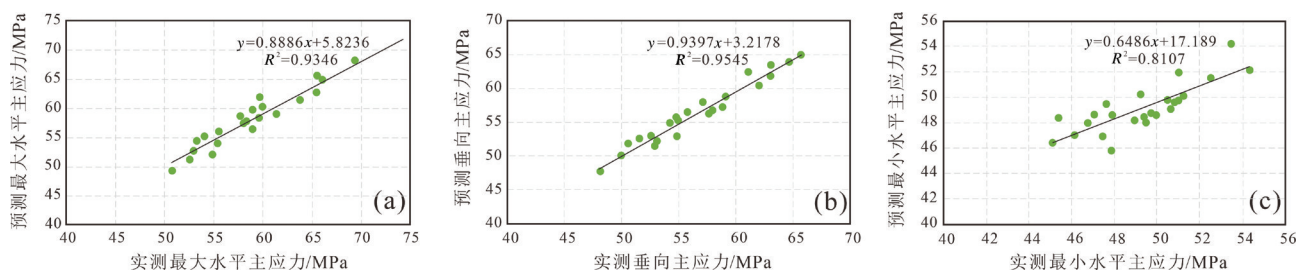

图7 须二段各小层实测与测井计算应力值对比图

a—须二段各小层实测与测井计算最大水平主应力对比图；b—须二段各小层实测与测井计算垂向主应力对比图；c—须二段各小层实测与测井计算最小水平主应力对比图

Fig. 7 Comparison of measured and logged stress values for each sub−layer in the second member of Xujiahe Formation

a−Comparison of measured and logged maximum horizontal principal stress in each sub−section of Xu−II; b−Comparison of measured and logged vertical principal stress in each sub−section of Xu−II; c−Comparison of measured and logged minimum horizontal principal stress in each sub−section of Xu−II

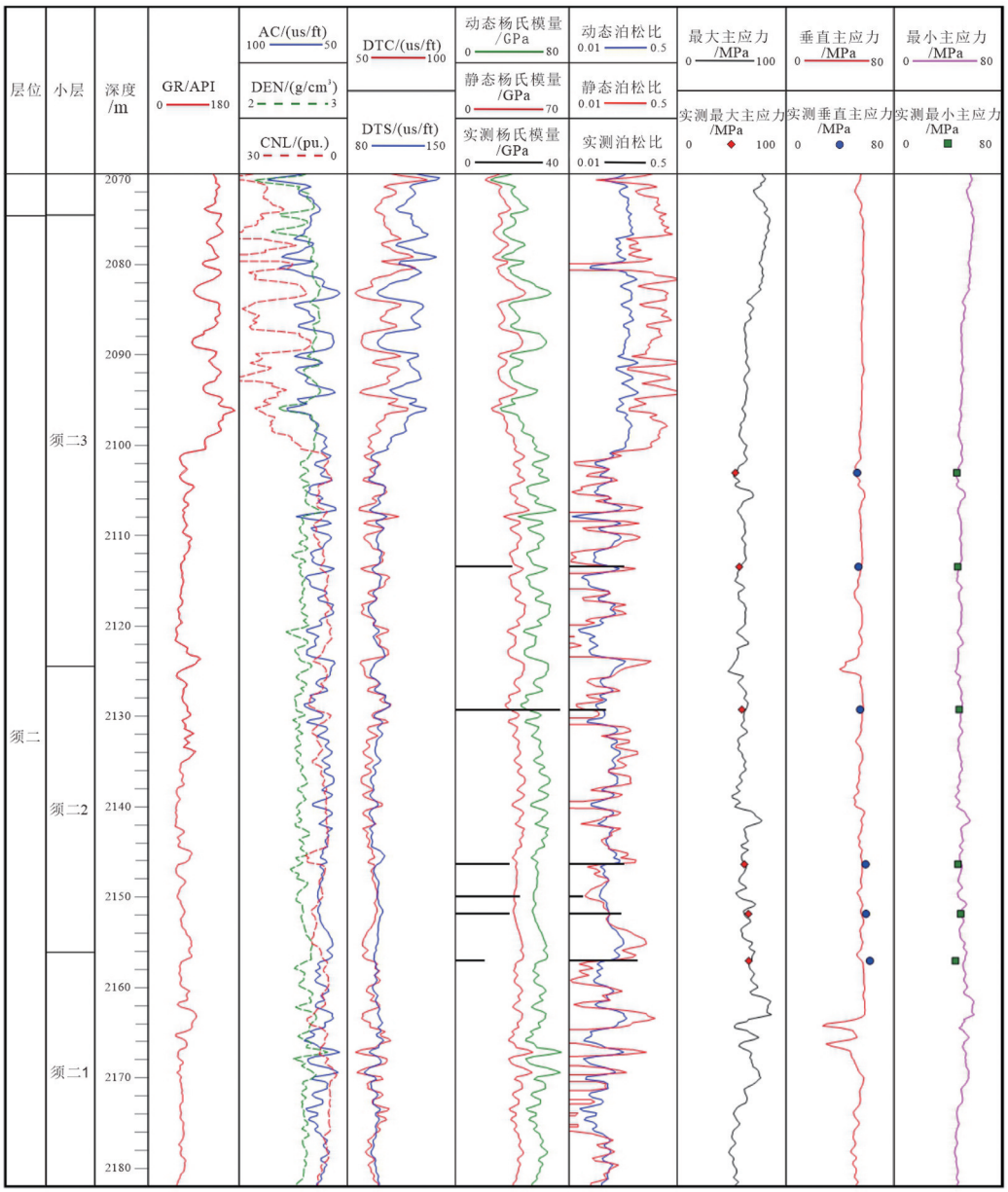

图8 HC001−69井须二段各小层岩石力学与地应力综合剖面

Fig.8 Integrated rock mechanics and in−situ stress profile of the second member of Xujiahe Formation of well HC001−69

合率均在81%以上,其中各小层的测井计算最大水平主应力值与实测最大水平主应力值的平均吻合率达到93.5%,各小层的测井计算垂向主应力值与实测垂向主应力值的吻合率均值为95.5%,而各小层的测井计算最小水平主应力值与实测最小水平主应力值的吻合率均值为81.1%(图7);同时,通过对利用上述方法建立的单井地应力测井解释剖面的分析(图8),可以发现随着埋深的增加,各向主应力值均有逐渐增加的趋势,3个方向主应力值之间大小关系满足 $\sigma_H < \sigma_v < \sigma_h$,也表现出走滑应力性质。测井解释结果与上述地应力实验测试结果基本一致,表明本次建立的三向应力测井解释模型的适用性较好。

5 地应力评价在致密砂岩气开发中的应用

5.1 纵向上压裂选层中的应用

利用Fracman软件模拟了储层应力为50 MPa,

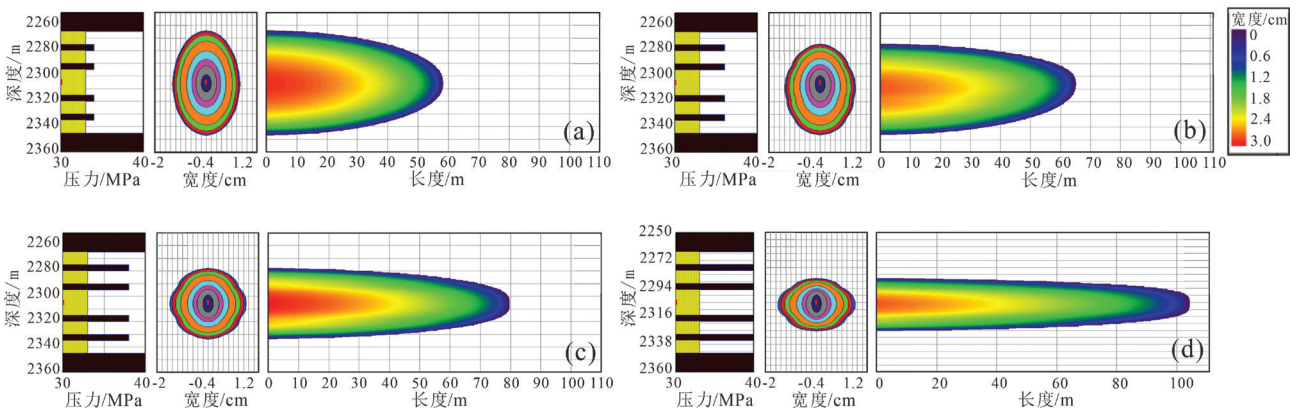

图9 不同内部应力差模拟水力裂缝扩展形态图

a—储层应力为50 MPa,隔层为51 MPa时裂缝扩展形态;b—储层应力为50 MPa,隔层为53 MPa时裂缝扩展形态;c—储层应力为50 MPa,隔层为55 MPa时裂缝扩展形态;d—储层应力为50 MPa,隔层为57 MPa时裂缝扩展形态

Fig.9 Simulation of hydraulic fracture extension patterns with different internal stress differences

a−Fracture extension pattern at 50 MPa for reservoir stress and 51 MPa for compartment; b−Fracture extension pattern at 50 MPa for reservoir stress and 53 MPa for compartment; c−Fracture extension pattern at 50 MPa for reservoir stress and 55 MPa for compartment; d−Fracture extension pattern at 50 MPa for reservoir stress and 57 MPa for compartment

隔层应力分别为51 MPa、53 MPa、55 MPa及57 MPa的情况下,水力裂缝的扩展形态(图9)。模拟结果表明,随着隔层应力的增大,裂缝的缝长逐渐变大而缝宽逐渐减小。说明储隔层应力差的增大抑制了裂缝的纵向延伸,而水力能量用于横向上的延伸,所以裂缝的缝长增加了。

同样,储层内部应力隔层的厚度也会对水力裂缝的扩展形态产生影响。随着隔层厚度的增大,裂缝高度逐渐减小,长度逐渐增大(图10)。说明应力隔层的厚度会较为明显地阻挡裂缝在纵向上的延伸,如需压开隔层则需较大的排量,加大了压裂难度。

以HC001−5−x3井须二段的水力压裂模拟为例,须二1亚段和须二3亚段在岩石力学和地应力剖面上相比于须二2亚段,存在较强且具有一定厚度规模的应力隔层,其应力剖面组合不利于水力裂缝的纵向扩展(图11)。且须二1亚段和须二3亚段实际模拟的压裂裂缝形态相比于须二2亚段,也出现水力裂缝

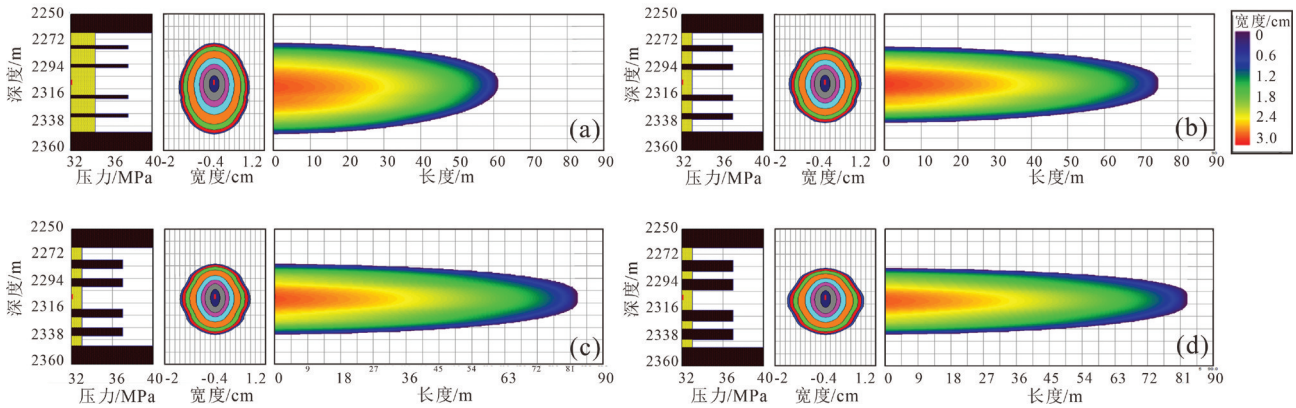

图10不同内部应力隔层厚度模拟水力裂缝扩展形态图

a—隔层为1 m时裂缝形态;b—隔层为3 m时裂缝形态;c—隔层为5 m时裂缝形态; d—隔层为7 m时裂缝形态

Fig. 10 Simulation of hydraulic fracture extension patterns with different internal stress compartment thicknesses

a−Crack pattern at a compartment thickness of 1 m; b−Crack pattern at a compartment thickness of 3 m; c−Crack pattern at a compartment thickness of 5 m; d−Crack pattern at a compartment thickness of 7 m

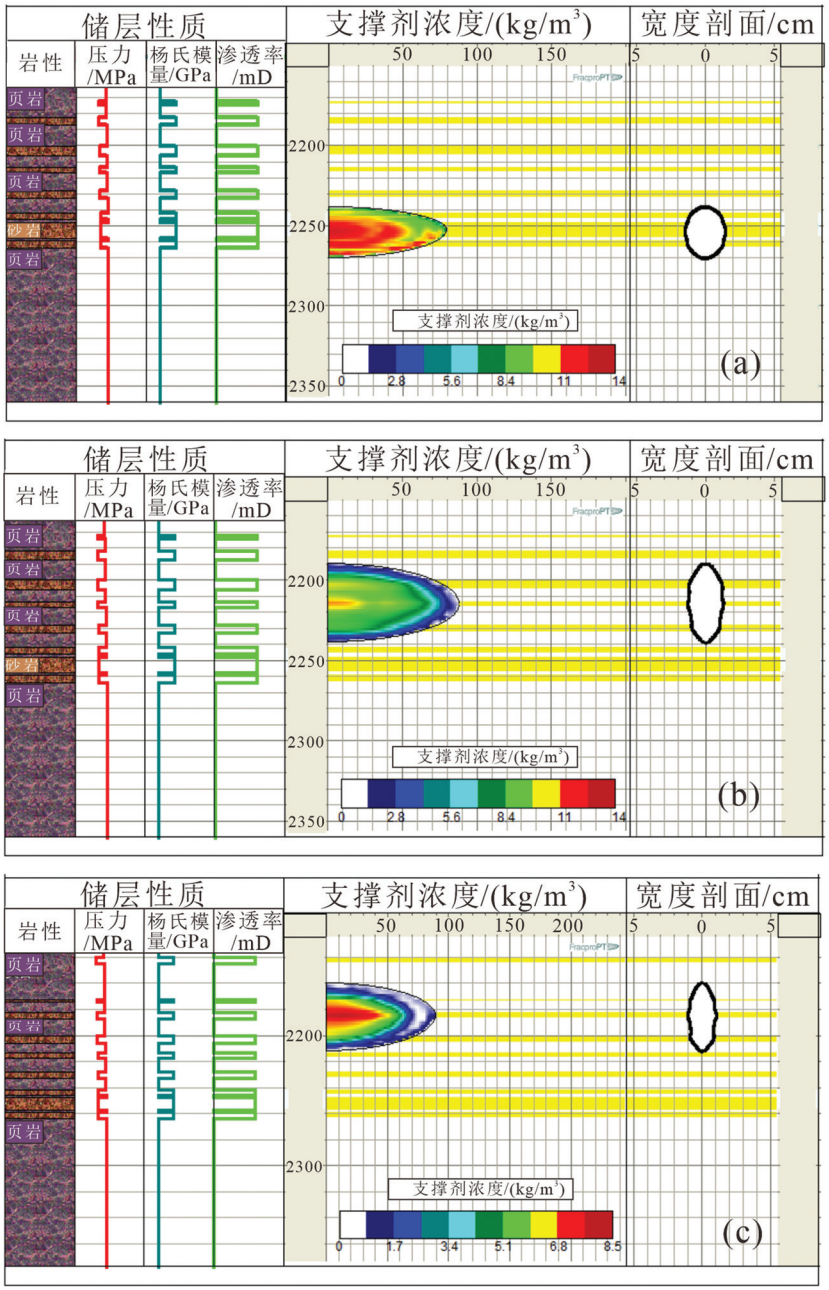

图11 HC001−5−x3须二段压裂裂缝形态模拟图

a—HC001−5−x3须二1亚段压裂裂缝形态模拟图;b—HC001−5−x3须二2亚段压裂裂缝形态模拟图;c—HC001−5−x3须二3亚段压裂裂缝形态模拟图

Fig. 11 Simulation of the fracture pattern of the second member of Xujiahe Formation fracture in well HC001−5−x3

a−Simulation of fracture morphology in the first subsection of Xu−II of well HC001−5−x3; b—Simulation of fracture morphology in the second subsection of Xu−II of well HC001−5−x3; c−Simulation of fracture morphology in the third subsection of Xu−II of well HC001−5−x3

的缝高有限且宽度较窄的情况。因此,须二2亚段的应力剖面组合更利于形成复杂体积缝网效果。

5.2 平面上压裂“甜点区”的优选

致密砂岩等非常规储层的物性较差,必须对其进行大规模全井段储层体积缝网改造才能获取经济产能(Mayerhofer et al.,2010)。研究表明,两向水平应力差越大,越不利于在井筒附近形成复杂的裂缝网络,且体积裂缝在长度上的展布范围增加、宽度上的展布范围减小,在水力压裂时易产生平直裂缝;反之,则易沿天然裂缝扩展形成复杂网状裂缝

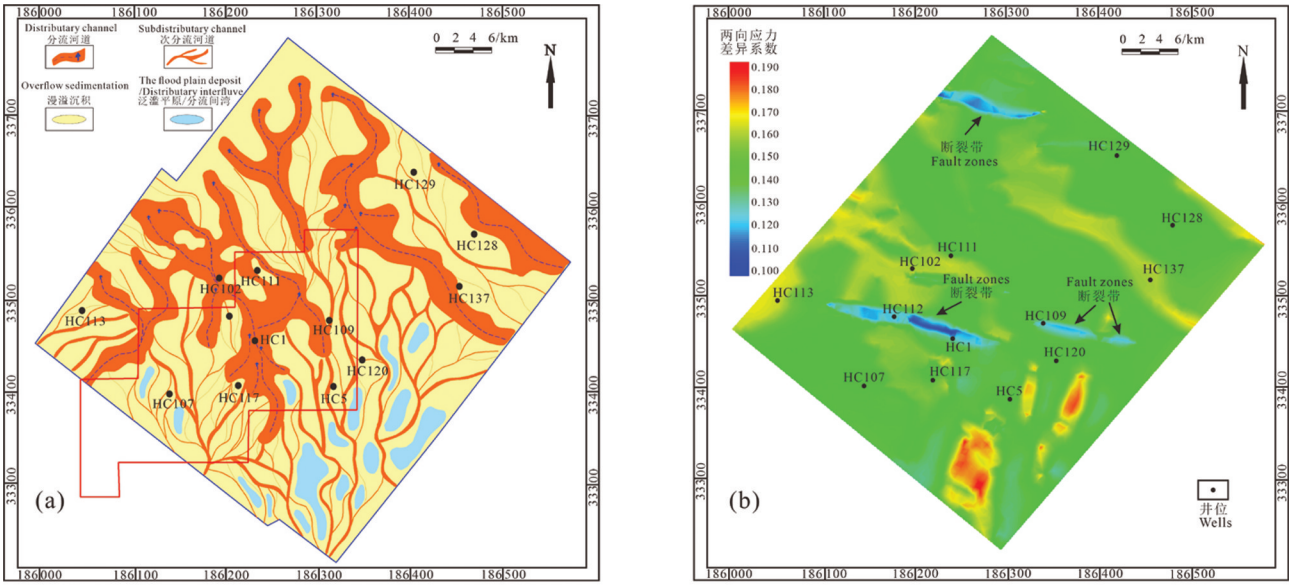

图12 须二2亚段两向应力差异系数分布图

a—须二段沉积相图;b—须二2亚段两向应力差异系数三维分布图

Fig. 12 Distribution of the differential coefficient of two-dimensional horizontal stress for the second subsection of Xu-II

a—Sedimentary facies map of the second member of Xujiahe Formation; b—Three-dimensional distribution of the differential coefficient of horizontal in-situ stress in both directions for the second subsection of Xu-II

(赵金洲等,2014;Zhang et al.,2019;宁文祥等,2021;史璨和林伯韬,2021)。目前,两向应力差异系数常被用来衡量水平地应力各向异性程度;两向应力差异系数(K_H)的定义为最大水平主应力与最小水平主应力之间差值与最小水平主应力的比值;两向应力差异系数在0~0.3时有利于形成裂缝网络,而当其大于0.5后则难以形成有效的裂缝系统;即K_H越小压裂后越容易形成复杂缝网,K_H越大压裂后越容易形成单一裂缝(Renshaw and Pollard,1994;曾治平等,2019;史璨和林伯韬,2021)。

基于数值模拟结果,认为HC地区须二2亚段的两向应力差异系数主要分布在0.10~0.190(图12),在分流间湾泥岩分布区的两向应力差异系数相对最高,分布在0.17~0.21,在断裂带内部的两向应力差异系数相对最低,分布在0.10~0.13,在主河道砂体分布区的两向应力差异系数相对较高,分布在0.16~0.18,而广阔的溢漫沉积过渡岩相分布区的两向应力差异系数则介于后两者之间,分布在0.13~0.16;综合考虑优质储层的分布区域,建议在HC地区中部HC102-HC111分布区进行水力压裂改造。

6 结 论

(1)实验测试结果表明,HC地区须二段致密砂岩气储层最大水平主应力值为50.77~75.65 MPa,均值为59.71 MPa;最小水平主应力值为45.37~54.31 MPa,均值为49.31 MPa;垂直主应力值为48.11~65.62 MPa,均值为56.53 MPa。三向应力具有最大水平主应力>垂向主应力>最小水平主应力的特征,属于Ⅲ类地应力类型,处于走滑应力状态。

(2)纵向上须二段由下至上,三向应力值逐渐减小。结合水压致裂、井壁崩落资料反演地应力大小,认为声发射测试结果误差较大,即差应变测试更适用于均质性致密砂岩储层。

(3)结合地应力大小对水力裂缝扩展形态的影响,纵向上HC地区须二段1、3亚段储隔层应力差较大,隔层厚度较厚,抑制裂缝纵向延伸,须二2亚段的应力剖面组合更利于形成复杂体积缝网效果;平面上在HC地区中部HC102-HC111分布区须二2亚段河道砂岩发育且两向应力差异系数相对较小,可作为致密砂岩气储层进行水力压裂改造的"甜点区"。

References

Cai Meifeng. 1993. Review of principles and methods for rock stress measurement[J]. Chinese Journal of Rock Mechanics and Engineering, 12(3): 275-283 (in Chinese with English abstract).

Cao Hui, Sun Dongsheng, Yuan Kun, Li Awei, Zhang Guanghan. 2020.

In− situ stress determination of 3 km oil− gas deep hole and analysis of the tectonic stress field in the southern Guizhou[J]. Geology in China, 47(1): 88−98 (in Chinese with English abstract).

Chen Nian, Wang Chenghu, Gao Guiyun, Wang Pu. 2021. Characteristics of in−situ stress field in the powerhouse area on the right bank of Baihetan based on stress polygon and borehole breakout method[J]. Rock and Soil Mechanics, 42(12): 3376−3384 (in Chinese with English abstract).

Ding Wenlong, Wang Xinghua, Hu Qiujia,Yin Shuai, Cao Xiangyu, Liu Jianjun. 2015. Progress in tight sandstone reservoir fractures research[J]. Advances in Earth Science, 30(7): 737− 750 (in Chinese with English abstract).

Fraser D, Gholami R, Sarmadivaleh M. 2021. Deformation rate analysis: How to determine in−situ stresses in unconventional gas reservoirs[J]. International Journal of Rock Mechanics and Mining Sciences, 146(7/8): 104892.

Guo Weijie, Gong Cheng, Li Jing. 2010. The measurements of geostress and the problems of geo−stress measurement[J]. Value Engineering, 29(25): 136−137 (in Chinese with English abstract).

Han Jun, Liu Hongtao. 2005. Application of differential strain analysis method on the study of in− situ stress direction[J]. Journal of Oil and Gas Technology, 27(2): 87−88, 95, 8(in Chinese with English abstract).

He Xiaodong, Ma Junxiu, Shi Shanzhi, Liu Gang, Tan Qiang. 2020. Core differential strain test of tight glutinite reservoir in Mahu oilfield[J]. China Offshore Oil and Gas, 32(3): 86−93 (in Chinese with English abstract).

Jayanthu S. 2019. Estimation of in−situ stress−experiemtnal trials on Kaiser effect and hydrofracturing tests[J]. Journal of Mines, Metals and Fuels, 67(6): 311−315.

Ji Zhijiu, Lu Guobin, Li Lan, 2009. Study on in− situ stress measurement method and engineering application[J]. Modern Mining, 25(11): 67−69 (in Chinese with English abstract).

Jiang Yongdong, Xian Xuefu, Xu Jiang. 2005. Research on application of Kaiser effect of acoustic emission to measuring initial stress in rock mass[J]. Rock and Soil Mechanics, 26(6): 946− 950 (in Chinese with English abstract).

Jing Feng, Liang Hecheng, Bian Zhihua, Liu Yuankun. 2008. Review of geo−stress measurement method and study[J]. Journal of North China University of Water Resources and Electric Power(Natural Science Edition), 29(2): 71−75 (in Chinese with English abstract).

Lehtonen A, Cosgrove J W, Hudson J A, Johansson E. 2011. An examination of in situ rock stress estimation using the Kaiser effect[J]. Engineering Geology, 124: 24−37

Li Guohui, Li Nan, Xie Jirong, Yang Jiajing, Tang Dahai. 2012. Basic features of large gas play fairways in the upper Triassic Xujiahe Formation of the Sichuan Foreland Basin and evaluation of favorable exploration zones[J]. Natural Gas Industry, 32(3): 15−21, 122−123 (in Chinese with English abstract).

Liang Chen. 2020. Theory and Numerical Analysis of a New Method of In− Situ Stress Measurement[D]. Wuhan: Hubei University of Technology (in Chinese with English abstract).

Liu R, Hao F, Engelder T, Shu Z, Yi J, Xu S, Teng C. 2019. Stress memory extracted from shale in the vicinity of a fault zone: Implications for shale− gas retention[J]. Marine and Petroleum Geology, 102: 340−349.

Liu Yaqun, Li Haibo, Jing Feng, Luo Chaowen, Chen Bingrui, Li Junru, Zhou Qingqing. 2007. Determination of in− situ stress by hydraulic fracturing tests on preexisting fractures considering stress gradient and its engineering application[J]. Chinese Journal of Rock Mechanics and Engineering, 26(6): 1145− 1149 (in Chinese with English abstract).

Liu Zekai, Chen Yaolin, Tang Ruzhong. 1994. Application of in− situ stress technology in oilfield development[J]. Petroleum Geology and Recovery Efficiency, 1(1): 48−56, 85(in Chinese).

Ma Rui. 2014. Application of ground stress in oil and gas exploration and development[J]. Science & Technology Information, 12(31): 55−58(in Chinese).

Mao H, Luo T, Lai F, Zhang G, Zhong L. 2019. Experimental analysis and logging evaluation of in−situ stress of mud shale reservoir——Taking the deep shale gas reservoir of Longmaxi Formation in western Chongqing as an example[C]// IOP Conference Series: Earth and Environmental Science, 384: 012129.

Mayerhofer M J, Lolon E P, Warpinski N R, Cipolla C L, Walser D, Rightmire C M. 2010. What is stimulated reservoir volume?[J]. SPE Production & Operations, 25(1): 89−98.

Nie Zhou. 2018. Study on the Reservoir Characteristics of the Second Member of Xujiahe Formation in the Central Sichuan Area[D]. Chengdu: Chengdu University of Technology (in Chinese with English abstract).

Ning Wenxiang, He Bai, Li Fengxia, Xie Lingzhi, Shi Aiping, He Qiang. 2021. Experimental study on fractures morphology of hydraulic fracturing in continental shale oil reservoir[J] Science Technology and Engineering, 21(18): 7505−7512 (in Chinese with English abstract).

Renshaw C E, Pollard D D. 1994. Are large differential stresses required for straight fracture propagation paths?[J]. Journal of Structural Geology, 16(6): 817−822.

Schmitt D R, Currie C A, Zhang L. 2012. Crustal stress determination from boreholes and rock cores: Fundamental principles[J]. Tectonophysics, 580:1−26.

Shen Haichao, Cheng Yuanfang, Wang Jingyin, Zhao Yizhong, Zhang Jianguo. 2008. Principal direction differential strain method for in− situ stress measurement and application[J]. Xinjiang Petroleum Geology, 29(2): 250−252 (in Chinese with English abstract).

Shi Can, Lin Botao. 2021. Principles and influencing factors for shale formations[J]. Petroleum Science Bulletin, 6(1): 92− 113 (in Chinese with English abstract).

Wang Chenghu, Gao Guiyun, Wang Hong, Wang Pu. 2020. Integrated determination of principal stress and tensile strength of rock based on the laboratory and field hydraulic fracturing tests[J]. Journal of Geomechanics, 26 (2): 167−174 (in Chinese with English abstract).

Wang Chenghu. 2014. Brief review and outlook of main estimate and measurement methods for in situ stresses in rock mass[J]. Geological Review, 60(5): 971− 991, 996, 992− 995 (in Chinese with English abstract).

Wang Hongwei. 2007. Study On Comprehensive Interpretation Method of Earth Stress In Different Tracts In Hailaer Oilfield[D]. Daqing: Daqing Petrolum Institute(in Chinese with English abstract).

Wang Pu, Wang Chenghu, Yang Ruhua, Hou Zhengyang, Wang Hong. 2019. Preliminary investigation on the deep rock stresses prediction method based on stress polygon and focal mechanism solution[J]. Rock and Soil Mechanics, 40(11): 4486− 4496 (in Chinese with English abstract).

Wang S, Han F, Bing Q. 2021. Application of In− situ Stress Calculation in Engineering[C]// IOP Conference Series: Earth and Environmental Science, 660(1): 012040.

Zeng Zhiping, Liu Zhen, Ma Ji, Zhang Chunlei, Li Jing, Liu Zhen, Sun Luning. 2019. A new method for fracrability evaluation in deep and tight sandstone reservoirs [J]. Journal of Geomechanics, 25(2): 223−232 (in Chinese with English abstract).

Zhang R, Hou B, Han H, Fan M, Chen M. 2019. Experimental investigation on fracture morphology in laminated shale formation by hydraulic fracturing[J]. Journal of Petroleum Science and Engineering, 177: 442−451.

Zhang Zhongyuan, Wu Manlu, Chen Qunce, Liao Chunting, Feng Chengjun. 2012. Review of in− situ stress measurement methods [J]. Journal of Henan Polytechnic University (Natural Science), 31(3): 305−310 (in Chinese with English abstract).

Zhao Gang, Dong Shier. 2009. The theory of the measurement of ground stress by hydraulic fracturing method and its application[J]. Shanxi Architecture, 35(36): 77− 78 (in Chinese with English abstract).

Zhao Jinghui, Gao Yuqiao, Chen Zhenlong, Guo Tao, Gao Xiaokang. 2021. Stress state of deep seam and its influence on development performance of CBM wells in South Yanchuan Block, Odors Basin[J]. Geology in China, 48(3): 785− 793 (in Chinese with English abstract).

Zhao Jinzhou, Li Yongming, Wang Song, Jiang Youshi, Zhang Liehui. 2014.Simulation of a complex fracture network influenced by natural fractures[J]. Natural Gas Industry, 34(1): 68−73 (in Chinese with English abstract).

Zhao Yajun, Meng Nannan. 2015. Review of in− situ stress measurement methods[J]. Inner Mongolia Coal Economy, (5): 209−210(in Chinese).

Zhao Zhengwang, Li Nan, Liu Min, Wang Xiaojuan, Wu Changjiang, Li Li. 2019. Origin of gas accumulation and high yield in tight gas reservoirs of Xujiahe Formation, Sichuan Basin[J]. Natural Gas Exploration and Development, 42(2): 39− 47 (in Chinese with English abstract).

Zheng Herong, Liu Zhongqun, Xu Shilin, Liu Zhenfeng, Liu Junlong, Huang Zhiwen, Huang Yanqing, Shi Zhiliang, Wu Qingzhao, Fan Lingxiao, Gao Jinhui. 2021. Progress and key research directions of tight gas exploration and development in Xujiahe Formation, Sinopec exploration areas, Sichuan Basin[J]. Oil & Gas Geology, 42(4): 765−783 (in Chinese with English abstract).

Zhu Hongquan, Zhang Zhuang, Nan Hongli, Ye Sujuan, Zhang Shihua, Wang Linghui. 2019. Reservoir formation and enrichment rules and exploration practices in overlying dense sandstone gas zones[J]. Natural Gas Industry, 39(S1): 9−16 (in Chinese).

附中文参考文献

蔡美峰. 1993. 地应力测量原理和方法的评述[J]. 岩石力学与工程学报, 12(3): 275−283.

曹慧, 孙东生, 苑坤, 李阿伟, 张光晗. 2020. 黔南地区~3 km 油气深孔地应力测量与构造应力场分析[J]. 中国地质,47(1): 88−98.

陈念, 王成虎, 高桂云, 王璞. 2021. 基于应力多边形与钻孔崩落的白鹤滩右岸厂房区地应力场特征研究[J]. 岩土力学, 42(12): 3376−3384.

丁文龙, 王兴华, 胡秋嘉, 尹帅, 曹翔宇, 刘建军. 2015. 致密砂岩储层裂缝研究进展[J]. 地球科学进展, 30(7): 737−750.

郭伟杰, 龚成, 李晶. 2010. 地应力测量方法及其需要注意的问题[J]. 价值工程, 29(25): 136−137.

韩军, 刘洪涛. 2005. 差应变分析法在地应力方向研究中的应用[J]. 石油天然气学报(江汉石油学院学报), 27(2): 87−88, 95, 8.

何小东, 马俊修, 石善志, 刘刚, 谭强. 2020. 玛湖油田致密砂砾岩储层岩心差应变实验[J]. 中国海上油气, 32(3): 86−93.

纪志久, 卢国斌, 李岚. 2009. 地应力测量方法及工程应用研究[J]. 现代矿业, 25(11): 67−69.

姜永东, 鲜学福, 许江. 2005. 岩石声发射Kaiser效应应用于地应力测试的研究[J]. 岩土力学, 26(6): 946−950.

景锋, 梁合成, 边智华, 刘元坤. 2008. 地应力测量方法研究综述[J]. 华北水利水电学院学报, 29(2): 71−75.

李国辉,李楠,谢继容,杨家静,唐大海.2012. 四川盆地上三叠统须家河组前陆大气区基本特征及勘探有利区[J]. 天然气工业, 32(3): 15−21,122−123.

梁晨. 2020. 一种新的地应力测量方法理论及数值分析[D]. 武汉：湖北工业大学.

刘亚群, 李海波, 景锋, 罗超文, 陈炳瑞, 李俊如, 周青春. 2007. 考虑应力梯度的原生裂隙水压致裂法地应力测量的原理及工程应用[J]. 岩石力学与工程学报, 26(6):1145−1149.

刘泽凯, 陈耀林, 唐汝众. 1994. 地应力技术在油田开发中的应用[J]. 油气采收率技术, 1(1): 48−56, 85.

马睿. 2014. 地应力在油气勘探开发中的应用[J]. 科技资讯, 12(31): 55−58.

聂舟. 2018. 川中地区须家河组二段储层特征研究[D]. 成都:成都理工大学, 1−4.

宁文祥, 何柏, 李凤霞,谢凌志, 史爱萍, 何强. 2021. 陆相页岩油储层水力压裂裂缝形态的试验[J]. 科学技术与工程, 21(18): 7505−7512.

沈海超, 程远方, 王京印, 赵益忠, 张建国. 2008. 主方向差应变地应力测量方法[J]. 新疆石油地质, 29(2): 250−252.

史璨, 林伯韬. 2021. 页岩储层压裂裂缝扩展规律及影响因素研究探讨[J]. 石油科学通报, 6(1): 92−113.

王成虎. 2014. 地应力主要测试和估算方法回顾与展望[J]. 地质论评, 60(5): 971−991, 996, 992−995.

王成虎, 高桂云, 王洪, 王璞. 2020. 利用室内和现场水压致裂试验联合确定地应力与岩石抗拉强度[J]. 地质力学学报, 26(2): 167−174.

王宏伟. 2007. 海拉尔油田不同区块地应力综合解释方法研究[D]. 大庆:大庆石油学院, 1−5.

王璞, 王成虎, 杨汝华, 侯正阳, 王洪. 2019. 基于应力多边形与震源机制解的深部岩体应力状态预测方法初探[J]. 岩土力学, 40(11): 4486−4496.

曾治平, 刘震, 马骥, 张春磊, 李静, 刘振, 孙鲁宁. 2019. 深层致密砂岩储层可压裂性评价新方法[J]. 地质力学学报, 25(2): 223−232.

张重远, 吴满路, 陈群策, 廖椿庭, 丰成君. 2012. 地应力测量方法综述[J]. 河南理工大学学报(自然科学版), 31(3): 305−310.

赵刚, 董事尔. 2009. 水压致裂法测量地应力理论与应用[J]. 山西建筑, 35(36): 77−78.

赵景辉, 高玉巧, 陈贞龙, 郭涛, 高小康. 2021. 鄂尔多斯盆地延川南区块深部地应力状态及其对煤层气开发效果的影响[J]. 中国地质, 48(3): 785−793.

赵金洲, 李勇明, 王松, 江有适, 张烈辉. 2014. 天然裂缝影响下的复杂压裂裂缝网络模拟[J]. 天然气工业, 34(1): 68−73.

赵亚军, 孟楠楠. 2015. 地应力测量方法综述[J]. 内蒙古煤炭经济, (5): 209−210.

赵正望, 李楠, 刘敏, 王小娟, 吴长江, 李莉. 2019. 四川盆地须家河组致密气藏天然气富集高产成因[J]. 天然气勘探与开发, 42(2): 39−47.

郑和荣, 刘忠群, 徐士林, 刘振峰, 刘君龙, 黄志文, 黄彦庆, 石志良, 武清钊, 范凌霄, 高金慧. 2021. 四川盆地中国石化探区须家河组致密砂岩气勘探开发进展与攻关方向[J]. 石油与天然气地质, 42(4): 765−783.

朱宏权, 张庄, 南红丽, 叶素娟, 张世华, 王玲辉. 2019. 叠覆型致密砂岩气区成藏富集规律与勘探实践[J]. 天然气工业, 39(S1): 9−16.